



# Intraplate tectonics: feedback between radioactive thermal weakening and crustal deformation driven by mantle lithosphere instabilities

Russell N. Pysklywec<sup>a,\*</sup>, Christopher Beaumont<sup>b</sup>

<sup>a</sup> *Department of Geology, University of Toronto, Toronto, ON, Canada M5S 3B1*

<sup>b</sup> *Department of Oceanography, Dalhousie University, Halifax, NS, Canada B3H 4J1*

Received 16 July 2003; received in revised form 12 January 2004; accepted 28 January 2004

## Abstract

Two-dimensional viscous–plastic numerical experiments show that weak radioactive crust may be susceptible to significant tectonic activity by the effect of Rayleigh–Taylor-type instability of the sub-crustal lithosphere below a continental interior. In particular, crust having a localized or regional enrichment of radioactive elements can respond to an underlying mantle lithosphere downwelling by initial subsidence then thickening and uplift owing to the positive feedback among thickening, heating, and weakening. Such models may later undergo orogenic deflation as spontaneous crustal extension/thinning and surface subsidence occur while mantle downwelling continues. Strong homogeneous crust subsides dynamically above mantle downwellings and undergoes essentially no internal deformation. A uniform distribution of radioactive elements through the crust, or a concentration at depth, is much more effective in causing thermal weakening of the crust and subsequent intraplate deformation than with radioactive material concentrated nearer the surface. For wide regions of high heat production in the crust the length scale of the intracrustal tectonic zone is controlled by the width of the mantle downwelling in contrast with narrow heat production regions which control their own length scale. In general, the numerical experiments demonstrate that the presence of radioactive elements may make the crust vulnerable to intraplate tectonic deformation and represent a primary control on the way the strength of the crust evolves during sub-crustal forcing. The results may explain first-order features of intraplate tectonics including the subsidence mechanism for intracontinental basins, orogenic crustal contraction, thickening and surface uplift, and subsequent extension and crustal deflation. The processes have particular implications for regions of high radioactive heat production and juvenile crust which would more likely have a higher concentration of radioactive elements in the lower crust.

© 2004 Elsevier B.V. All rights reserved.

*Keywords:* intraplate tectonics; Rayleigh–Taylor instabilities; radioactive heating; numerical modeling; mantle lithosphere

## 1. Introduction

Although large-scale tectonic deformation of the lithosphere is largely confined to the plate boundary regions, significant deformation can

\* Corresponding author. Tel.: +1-416-978-4852;  
Fax: +1-416-978-3938.  
E-mail addresses: [russ@geology.utoronto.ca](mailto:russ@geology.utoronto.ca)  
(R.N. Pysklywec), [chris.beaumont@dal.ca](mailto:chris.beaumont@dal.ca) (C. Beaumont).

also occur in plate interiors. The continental plates contain sedimentary basins, for example, that have developed far from plate margins. Similarly, episodes of intraplate crustal uplift and orogeny are evident in the geological record. The tectonic evolution of these intraplate features must either be caused by forces transmitted through the lithosphere from plate boundaries or by a mechanism that is independent of plate boundary forces. Here we investigate the second type of mechanism.

Recent geodynamic work suggests that crustal tectonic events in a continental interior may be intimately linked to large-scale dynamics in the underlying mantle. For example, it has been shown that large-scale deflections of the lithosphere may be a result of underlying mantle convective flow. That is, flow in the viscous mantle can induce significant normal stresses at the surface, which may lead to transient events of surface uplift/depression or ‘dynamic topography’ [1,2]. This link between surface topography and mantle dynamics has provided an important mechanism that explains various episodes of observed large-scale continental uplift [3,4] and subsidence [5–8]. However, models of these processes generally adopt only a rudimentary thermal lithosphere and, in particular, neglect the presence of a deformable crust. Moreover, the dynamic topography is computed a posteriori as the instantaneous response of the lithosphere to the computed normal component of hydrodynamic stress at the top surface of the mantle flow models. Thus, this type of approach precludes the investigation of time-dependent lithospheric deformation induced by flow stresses tangential to the base of the lithosphere.

Numerical modeling applied to tectonics on Venus provided some of the first insights into the coupled interaction between mantle convection and crustal dynamics [9–12]. One of the common findings among these studies was that, depending on the rheology of the overlying crust, mantle downwelling may drive crustal thickening (and inferred plateau formation), rather than subsidence. Since plate tectonics is not active on Venus, it was suggested that such a process may be important for driving crustal deformation and uplift.

A similar mechanism may be responsible for inducing crustal tectonics in intraplate regions on Earth. Various studies have considered crustal deformation and the evolution of surface topography during episodes of gravitational instability of the lithosphere [13–15]. Neil and Houseman [15] calculate the influence of isothermal Rayleigh–Taylor (RT) instabilities of layered linear viscous lithosphere models on crustal deformation. They show that mantle lithosphere (i.e., sub-crustal lithosphere) downwellings can induce continental crust to contract and thicken, and that such events may be interpreted as intraplate orogenies which may occur without any horizontal plate boundary forcing. However, the rheology of the mantle lithosphere and crust must be relatively weak (viscosity of  $\sim 10^{21}$  Pa·s for the mantle lithosphere; and  $< 13$  times greater than this for the crust) for viscous RT instability and crustal thickening to occur [15].

The coupled crustal response to thermal downwelling in a convecting mantle shows similar results. Zhong [16] considered relaxation of crustal topography in a crust–mantle model using non-linear visco-elastic rheologies. The results similarly show that time-varying over-compensated topography can develop under the influence of sub-lithospheric loading, but the analyses impose a constant mantle buoyancy load and consequently neglect the influence of time-dependent convection in the underlying mantle. Three-dimensional isoviscous simulations of time-dependent mantle convection that include a buoyant overlying crust demonstrate variable crustal accumulation and thickening above regions of downwelling mantle flow [17,18]. The resulting high positive topography is not in (Airy) isostatic equilibrium, as the crustal thickening is dynamically supported by the time-varying mantle fluid flow. Thermal convection models which test the response of various crustal rheologies (Newtonian viscous) to time-dependent flow find that a crustal viscosity of  $< \sim 10^{23}$  Pa·s is required for the crust to deform appreciably by flow-induced shear stresses at the base of the crust [19].

In general, these studies suggest that intraplate crustal tectonics may be driven by mantle flow

dynamics if the crust is relatively weak. However, modern thermally stable continental crust as a whole is strong (e.g., [20]). This is clear from the rigid behavior of the plates which tend to resist large-scale deformation except in high stress regimes, such as plate boundaries. Localized weakening of the crust, however, may make it susceptible to focussed deformation in a plate interior. In particular, regions in which crustal radioactive heat production is anomalously high can be significantly weaker than normal crust, and as a result may be vulnerable to deformation driven by underlying mantle forcings.

As an example, Australia represents a region of high past and present heat flow having a relative abundance of radioactive heat-producing elements in its crust [21]. Furthermore, since the Paleoproterozoic the continent has experienced a significant number of episodes of intraplate tectonic activity (e.g., [22–25]). It has been proposed that there may be a causal relationship between the radioactive heating/weakening and certain phases of intracratonic deformation [21,26–28]. In addition, changes in the distribution of the radioactive materials during progressive evolution of the crust may result in various phases active/inactive tectonism [28].

Here we use thermomechanical numerical models to consider the evolution of intraplate crust having regions of locally enriched radioactive heating during an episode of mantle downwelling flow. The purpose is to investigate the feedback between thermal weakening of the radioactive crust and crustal deformation in response to a time-dependent mantle forcing. In particular, as a driving mechanism we model the development of RT-type instability of the mantle lithosphere having temperature-dependent density and temperature-dependent, power-law viscosity.

We conduct experiments having various configurations of radioactive heating in the model crust. The evolution of surface topography is tracked in the models as a primary observable associated with the crustal response to the underlying mantle flow. In addition, the style of internal deformation of the crust is investigated in detail to determine how time-dependent variations in crustal strength control its behavior.

## 2. Numerical experiments

### 2.1. Model set-up

Numerical geodynamic experiments were conducted to investigate the coupled evolution of the lithosphere and mantle during an episode of RT-type instability of the mantle lithosphere. The equations governing the thermomechanical behavior of incompressible viscous–plastic media in plane strain are solved using arbitrary Lagrangian–Eulerian (ALE) finite element techniques [29].

The model is set up as an idealized representation of the upper mantle and crust (Fig. 1; Table 1). The lithosphere is composed of a 30 km thick buoyant crust and a 120 km thick region of mantle lithosphere, and the remainder comprises the sub-lithospheric mantle. The uppermost 30 km is a chemically distinct, buoyant crust. The crust is defined as a frictional plastic material that also deforms below the yield stress with a non-linear temperature-dependent viscous flow law based on the experimental results of Gleason and Tullis [30] for wet quartzite (Fig. 1). A nominal value of  $\phi=15$  is used for the angle of internal friction that determines the plastic yield stress. While there are large associated uncertainties, this value is an estimate (e.g., implicitly assuming the influence of approximately hydrostatic pore fluid pressure) based on applied Coulomb wedge and crustal modeling [31,32].

The rheology of the mantle in the model is also plastic–viscous with thermally activated power-law creep, using viscous flow parameters for a dry olivine based on the experimental results of Hirth and Kohlstedt [33]. Although the model mantle is chemically homogeneous, rheological differentiation (i.e., into lithospheric and asthenospheric mantle regions) occurs in the models as a result of dynamic variations in the system ( $T$ ,  $\dot{\epsilon}$ ). In particular, due to the temperature dependence of rheology, a stronger mantle lithosphere region develops in that portion of the mantle with a temperature of  $<1350^{\circ}\text{C}$ . The initial thermal structure for the model was calculated based on a conductive equilibrium geotherm, and the base of the lithosphere (i.e., which we define with the  $1350^{\circ}\text{C}$

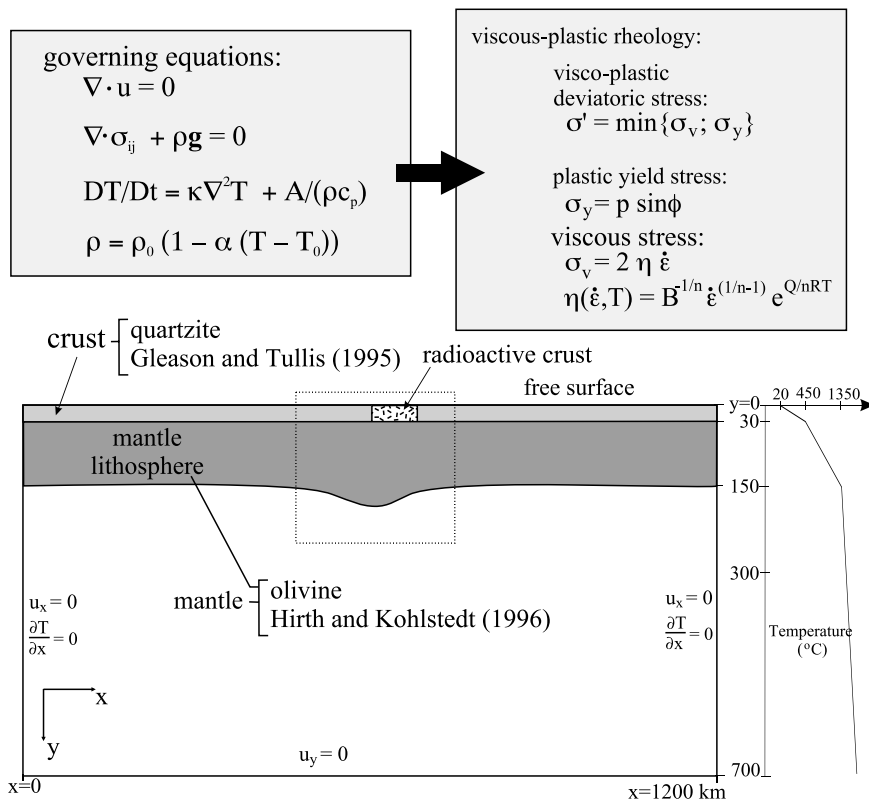


Fig. 1. Initial geometry of the full solution space for the numerical model. The buoyant model crust (light gray) is a chemically distinct material from the underlying mantle lithosphere (dark gray) and the hotter, weaker underlying mantle (asthenosphere). Power-law viscous parameters ( $B$ ,  $n$ ,  $Q$  – see Table 1) for the crust are based on experimental results for wet quartzite [30], and dry olivine for the mantle [33]. The position of the block of radioactive crust for the first numerical experiment is denoted. Undisturbed geotherm (away from radioactive region; see text) is plotted at right. Solution space has a free top surface, reflecting boundary conditions on the side walls, and no material flux through the bottom boundary. Dashed box shows zoomed region of model in Fig. 2. Governing equations for the system and formulation of viscous-plastic rheology in the model are shown. In these expressions  $\rho$ ,  $\mathbf{u}$ , and  $T$  represent the fields of density, velocity, and temperature, respectively. The variables  $g$ ,  $A$  and  $t$  are gravitational acceleration, rate of internal heat production per unit volume, and time (see Table 1 for definition and values of remaining model parameters). In the viscous-plastic model the deviatoric stress,  $\boldsymbol{\sigma}'$ , is determined at each computational node as the lesser value of either a plastic yield stress  $\boldsymbol{\sigma}_y$  or a viscous stress  $\boldsymbol{\sigma}_v$ ; where  $p$  is the pressure,  $\dot{\boldsymbol{\epsilon}}$  is the second invariant of the strain rate, and  $\eta$  is effective viscosity.

isotherm) was set at a depth of 150 km (Fig. 1). This initial temperature profile was laterally continuous across the computational domain, except where regions of radioactive heating were introduced into the crust (see below).

Deformation in the model is driven by the chemical and thermal buoyancy anomalies of the crust and mantle materials. A thermal perturbation (of width 200 km, and amplitude 15 km) to the base of the mantle lithosphere is introduced to

initiate an RT downwelling in the center of the model (Fig. 2;  $t = 0$ ). This perturbation is not the minimum that would drive the finite instability of the mantle lithosphere. Rather than examining the parameters that control the growth of the instability as has been considered in previous studies [34–37], we assume that a sufficient perturbation exists to cause onset of finite instability. Such a perturbation may arise, for example, from in-plane plate compression leading to minor contrac-

tion of the lithosphere, or inherent thermal instability of the thermal boundary layer in the broad-range mantle convective system.

A free surface at the top of the numerical model allows us to track directly the deformation of the crust and evolution of topography. The side walls and bottom boundary of the solution space are free slip; with zero tangential stress and no material transfer across the boundaries. This condition is not overly restrictive because we limit our investigations to the early stages of the model evolution when the influence of the bottom boundary on the deformation of the lithosphere is minimal. The temperature at the top and bottom of the box are held fixed at 20 and 1820°C, respectively; the heat flux out the side boundaries is zero. In the experiments we maintain a nearly constant geothermal heat flux into the base of the lithosphere by significantly increasing the thermal conductivity of the sub-lithospheric mantle (to 41 W/m/K; Table 1). The high thermal conductivity in the sub-lithospheric mantle maintains a vertical heat transport in this region that essentially is equivalent to a convecting mantle, without the need to model finite amplitude thermal convection. This effectively keeps the sub-lithospheric mantle close to the adiabatic geothermal gradient and allows us to isolate the effect of the RT instability on the crust from other thermal convective boundary layer instabilities.

The accuracy of the computational code has been verified by a series of benchmarking tests. Detailed analyses of the growth of RT instabilities indicate that our numerical formulation is in close agreement with other numerical and analytical

studies [35,38]. In addition, the development of free surface topography in the code is consistent with mantle flow-induced topography derived from other free surface models [39] and a posteriori calculations from fixed surface models [40].

## 2.2. Evolution of surface topography: influence of a region of radioactive crust

In this first series of experiments, we consider the influence of a region of high radioactive heat production in the crust on the crustal response to RT downwelling. In the first model we consider an end-member case in which the crust is given a high radioactive heat production of  $A = 5 \mu\text{W}/\text{m}^3$ , while the rest of the crust has no heat production. This 100 km wide radioactive block extends through the full thickness of the crust and is offset from the center of the mantle lithosphere perturbation (Fig. 1). The offset is chosen such that one side of the radioactive block is above the center of the downwelling. The asymmetry of the surface topographic response above the downwelling will therefore provide a general comparison of the relative response of radioactive and non-radioactive crust.

To generate the initial thermal structure of the model including the radioactive crust, a ‘thermal equilibration’ phase was run until the radioactive crust reached a state of conductive equilibrium. For this, the thermal state of the model was advanced while preventing material motion (i.e., thermal advection) and prior to introducing the RT instability.

Fig. 2 ( $t = 0$  Myr) shows the state of the ther-

Table 1  
Modeling parameters/properties

	Parameter	Crust	Mantle lithosphere	Sub-lithospheric mantle
$B$	viscosity parameter	$1.1 \times 10^{-15} \text{ Pa}^{-n}/\text{s}$	$4.85 \times 10^{-15} \text{ Pa}^{-n}/\text{s}$	$4.85 \times 10^{-15} \text{ Pa}^{-n}/\text{s}$
$n$	power exponent	4.0	3.5	3.5
$Q$	activation energy	223 kJ/mol	535 kJ/mol	535 kJ/mol
$\phi$	internal angle of friction	15°	15°	15°
$\rho_0$	reference density	$2.8 \times 10^3 \text{ kg}/\text{m}^3$	$3.3 \times 10^3 \text{ kg}/\text{m}^3$	$3.3 \times 10^3 \text{ kg}/\text{m}^3$
$T_0$	reference temperature	500°C	800°C	800°C
$\alpha$	coeff. of thermal expansion	$3.0 \times 10^{-5} \text{ K}^{-1}$	$2.0 \times 10^{-5} \text{ K}^{-1}$	$2.0 \times 10^{-5} \text{ K}^{-1}$
$c_p$	specific heat	1250 J/kg/K	1250 J/kg/K	1250 J/kg/K
$k$	thermal conductivity	2.25 W/m/K	4.86 W/m/K	41.0 W/m/K

mal–mechanical model following the end of the thermal equilibration phase. This initial state assumes the presence of a mantle lithosphere perturbation beneath a long-lived, pre-existing region of anomalous crustal heat production. At  $t=0.25$  Myr, the initial thermal and lithospheric boundary perturbation has developed into a dense mantle lithosphere root that is descending into the mantle as a gravitational instability. Elevated isotherms indicate relative heating in the radioactive crust while isotherms in the sub-crustal root are depressed as the relatively colder material sinks.

The unstable root descends quickly and sets up significant flow in the low-viscosity sub-lithospheric mantle, reaching velocities  $\sim 2$  cm/yr ( $t=0.75$  Myr). Adjacent lower mantle lithosphere material is laterally entrained into the developing RT downwelling. Between  $t=0.75$  and 3.25 Myr the flow is at its most vigorous as the initial root of mantle lithosphere mantle drips into the mantle. Lithospheric deformation occurs primarily in the lowermost regions of the mantle lithosphere. This is a result of the temperature-dependent non-linear viscosity of the mantle material which promotes more localized flow in the hot regions at the base of the lithosphere.

By  $t=10$  Myr there is continued, but less pronounced downwelling of the mantle lithosphere beneath the radioactive region of the crust. The main convective instability event has occurred but some downwelling is maintained by a smaller, convectively cooled remnant root.

The profiles of surface topography across the full width of the solution space are plotted for each of the time frames shown in Fig. 2 (Fig. 3). During the initial stages ( $t=0.25$ – $0.75$  Myr), a negative surface topography develops above the non-radioactive crust above the developing RT instability, with positive topography on the

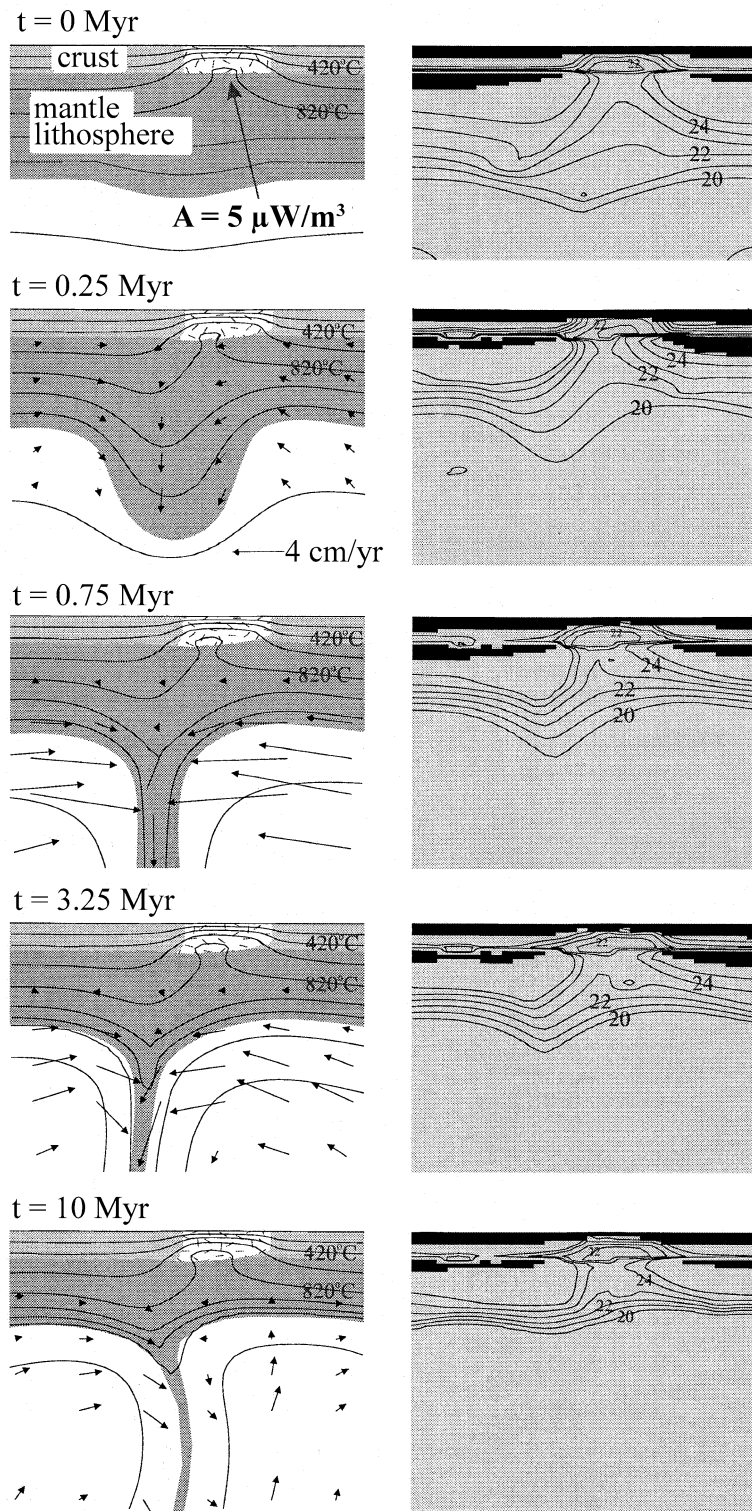
flanks. This topography is essentially the response of the strong crust to the normal stresses induced at the surface by the central mantle lithosphere downwelling and associated mantle return flow (Fig. 2). However, the symmetry of the topography is broken by a distinct, short wavelength perturbation at the location of the block of radioactive crust. By  $t=3.25$  Myr, this small perturbation has grown to a distinct positive spike in topography. At the same time, the surface subsidence adjacent to the spike has reached its maximum amplitude of  $\sim 500$  m during the most vigorous phase of RT downwelling. At  $t=10$  Myr the surface topography is dominated by the high elevation feature of  $\sim 750$  m amplitude above the region of radioactive crust. Topography variations in the unperturbed portions of the lithosphere, away from the zone of convergence are caused by the time-dependent mantle flow (which may have a relatively more important effect in these closed box models than would be expected in natural systems).

This distinctly time-dependent evolution of surface topography may be understood by considering the effect of the underlying flow stresses on the heterogeneous crust. The vertical component of hydrodynamic stress associated with the evolving downwelling mantle lithosphere instability causes time-varying regional subsidence of the crust. This ‘dynamic topography’ will be sustained only as long as there is active sub-crustal flow. A horizontal forcing also acts on the crust as a result of the RT mantle lithosphere downwelling which causes horizontal shortening of the crust.

Although most of the lithospheric deformation occurs in the lowermost mantle lithosphere (Fig. 2), the RT instability also induces significant stresses in the upper lithosphere. In general these flow-driven shear stresses will deflect the crust

---

Fig. 2. Progressive evolution of the first model showing development of RT mantle lithosphere instability and crustal deformation;  $t$  is time relative to onset of numerical experiment. In the left column, material regions (shaded) and instantaneous velocity vectors are plotted. Contours of temperature following thermal equilibration are superimposed; contour interval is  $200^\circ\text{C}$ , starting at  $20^\circ\text{C}$  at the surface. In the right column, contours of the log of effective viscosity,  $\log(\eta)$  ( $\eta$  as defined in Fig. 1) at intervals of one for the corresponding times. Shading marks material that is in the plastic (dark) or viscous (light) regime. Effective viscosity in the model is clearly reduced in regions of radioactive heat production; radioactive crustal heating is also responsible for minor temperature inversion in the lithosphere.



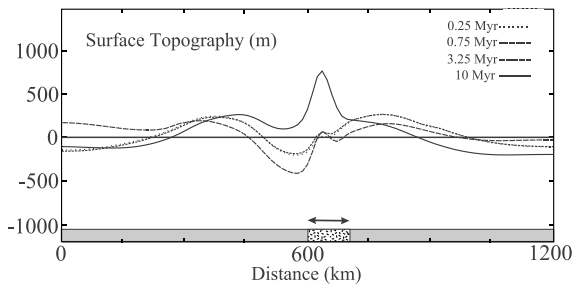


Fig. 3. Plot of surface topography across the first model with  $A=5 \mu\text{W}/\text{m}^3$  at the four time frames shown in Fig. 2. A stylized crust (not to vertical scale) is illustrated to show the location and configuration of the enriched radioactive region in the crust.

downward but are not sufficient to cause deformation of the relatively strong nominal quartz-rich crust. In this case, the response of the crust will be governed by the instantaneous vertical viscous flow stresses. However, in a region where radioactive heating results in local weakening of the crust and uppermost mantle, the basal shear stresses associated with the sub-crustal flow can cause appreciable internal deformation of the crust. In the case of the radioactive crust located in a region above the mantle lithosphere downwelling, flow-induced convergence will thicken the hot, susceptible crust. This, in turn, will result in surface uplift which has dynamical and long-term isostatic components, the latter from the net crustal thickening. If the thickening and uplift are sufficient, there may be a net positive surface topography despite a simultaneous downward mantle dynamical forcing.

The first-order character of the crustal deformation is evident in the deformed radioactive crust region in Fig. 2. Essentially, the ductile lower crust, weakened by radioactive heating, is entrained horizontally towards the mantle lithosphere downwelling, and as a whole the radioactive block undergoes shortening. Later, we examine in more detail the nature of this flow-induced crustal deformation.

In Fig. 4a we show the evolution of surface topography above a model crust that does not contain a region of radioactive heating. In all other respects, the experiment is the same as the previous model. The formation of the RT instability

in this homogeneous crust model is essentially the same (i.e., in timescale and thermal character) as in Fig. 2. A negative topography develops above the descending RT instability, and reaches a maximum depression of  $\sim 800$  m by  $t=3.25$  Myr. At  $t=10$  Myr, although there is still surface subsidence at the center of the solution space, the magnitude is decreased as the initial mantle lithosphere root detaches but more subdued downwelling flow continues. Clearly the evolution of surface topography is very much different in the model without local radioactive heating. The strength of the homogeneous crust and uppermost mantle prevents significant internal deformation by flow-induced shear stresses lower in the lithosphere, so the dynamic vertical response dominates the surface topography signal.

The rate of heat production in an enriched radioactive region of the crust may also be expected to have a significant effect on the crustal response

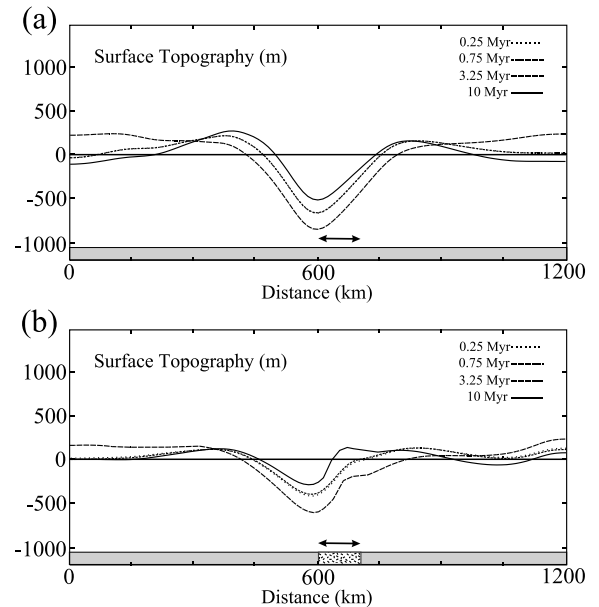


Fig. 4. Plot of surface topography at four time intervals for: (a) model in which radioactive region has been removed from the crust. The arrow indicates the lateral position of the radioactive block in the previous experiment. (b) Model with a radioactive block extending through the full thickness of the crust with a reduced heat production of  $A=2.5 \mu\text{W}/\text{m}^3$ .

to the sub-lithospheric dynamics. The value of  $A = 5 \mu\text{W}/\text{m}^3$  may correspond to continental regions of unusually high radioactive heat production (e.g., see discussion related to Mt. Isa region, below). In Fig. 4b, we show the results of an experiment that is the same as the original model (Fig. 2) except that the amount of radioactive heat production in the anomalous crustal block has been reduced to  $A = 2.5 \mu\text{W}/\text{m}^3$ . Initially the crust subsides above the mantle lithosphere instability. A subtle surface uplift gradually develops at the location of the radioactive region, but neither surface subsidence nor uplift strongly dominate by  $t = 10$  Myr. This represents an intermediate model to the end-member cases where crustal thickening and uplift (Fig. 3) or dynamic subsidence (Fig. 4a) dominate the crustal response.

### 2.3. Vertical distribution of radioactive heating and evolution of surface topography

The initial model assumed that radioactive heating was distributed uniformly through the entire thickness of crust in the radioactive region (Fig. 2). This situation may be applicable for juvenile, undifferentiated crust, but in evolved crust common to most continental interiors, radioactive elements are generally concentrated near the surface [41]. In Fig. 5 we show the results of two numerical experiments which considered two alternative configurations of crustal radioactive heating.

In Fig. 5a, the block of radioactive crust ( $A = 5 \mu\text{W}/\text{m}^3$ ) is limited to the lower half of the crust. Otherwise, the model set-up is unchanged and the evolution of the sub-crustal flow is the same as in Fig. 2. A negative surface topography develops above the mantle lithosphere downwelling during the initial stages of the model ( $t = 0.25$ – $3.25$  Myr), but a localized elevation high is clearly developing above the radioactive block. By  $t = 10$  Myr, the topography is dominated by this uplift. As in the original model with radioactive heating (Fig. 3), the thermally weakened crust is able to deform by the effect of the mantle lithosphere flow, and the subsequent crustal thickening and uplift overcome the dynamic subsidence of the crust. Although the surface uplift is appreciable in this

model, it is more subdued than in Fig. 3. This is obviously due to the smaller region of radioactive heat production and, hence, reduced integrated heating/weakening over the entire crust and uppermost mantle.

A similar experiment was conducted in which the  $A = 5 \mu\text{W}/\text{m}^3$  radioactive region was restricted to the top 15 km of the crust (Fig. 5b). In this case, the surface topography above the downwelling remains negative throughout the model run. With this configuration of radioactive heating, the whole crust and uppermost mantle remain relatively cool and strong and resist deformation induced by mantle lithosphere flow-induced tractions. Instead, the surface topography is controlled by the normal component of the hydrodynamic stresses, and their effect on the strong crust. The pair of experiments demonstrate that, as expected, deeply buried sources of radioactive heat are much more effective at heating (and weakening) the crust than those located near the surface.

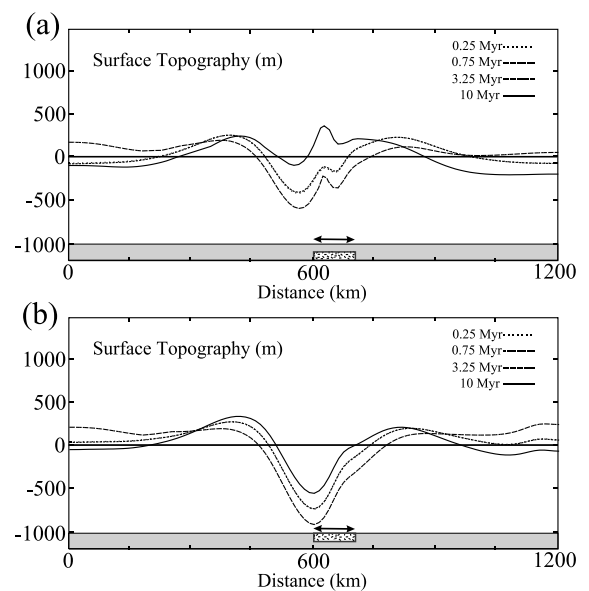


Fig. 5. Plot of surface topography at four time intervals for: (a) model with a radioactive block in the lower half (15 km) of the crust with heat production  $A = 5 \mu\text{W}/\text{m}^3$ ; (b) model with a radioactive block in the top half (15 km) of the crust with heat production  $A = 5 \mu\text{W}/\text{m}^3$ .

#### 2.4. Feedback between crustal deformation and radioactive thermal weakening

The feedback between radioactive thermal weakening and deformation of the crust is a primary process in controlling the response of the crust to the mantle dynamic forcing. Here, we consider in more detail this interaction during evolution of the crust–mantle system.

An alternate series of models was developed in which the initial mantle lithosphere perturbation (i.e., as shown in Fig. 2,  $t=0$  Myr) and crustal radioactive region were placed at the left-hand side of the solution space (Fig. 6a). This configuration takes advantage of the mirror symmetry of the model, allowing for a greater numerical resolution and facilitating interpretation by effectively keeping the locus of deformation stationary. The radioactive block,  $A=5\ \mu\text{W}/\text{m}^3$ , is situated in the lower half of the crust (i.e., lower 15 km) and has a half-width of 50 km. Besides the modification of geometry, all other parameters of the model, such as material rheologies, initial geotherm, thermal perturbation, and boundary conditions are the same as shown in Fig. 1. An initial thermal equilibrium phase is included.

The mantle lithosphere instability develops as a downwelling at the left boundary of the model on a timescale similar to that shown in Fig. 2. Initially, the downwelling induces contraction and thickening in the crust and entrains the thermally weakened ductile crust towards the center of the downwelling (Fig. 6b). This is similar to the lower crustal lateral entrainment evident in Fig. 2, ex-

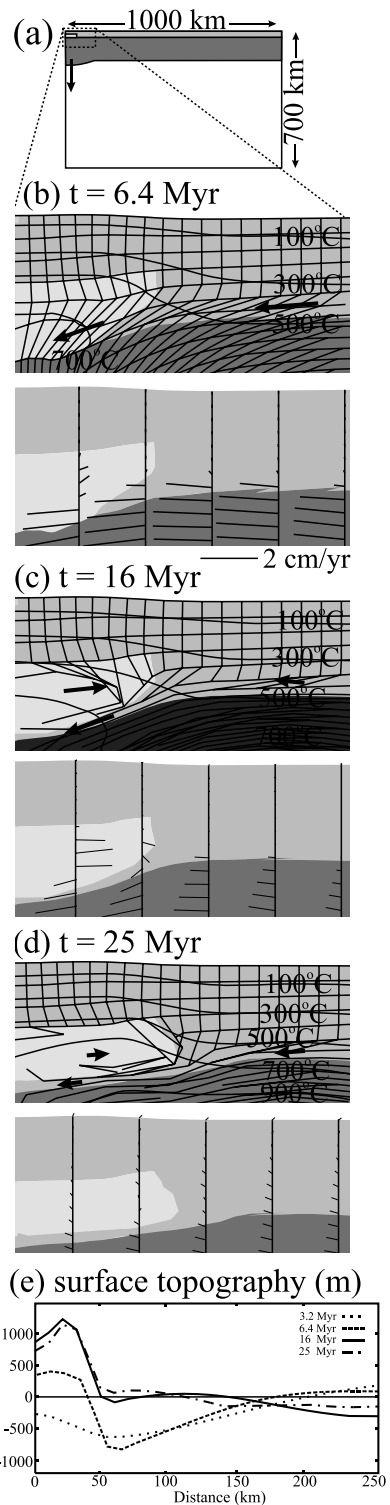


Fig. 6. Progressive deformation of crust in model with gravitational instability and radioactive crust at the left boundary of the solution space. (a) Initial model geometry; 15 km thick, 50 km wide radioactive region in lower crust (light gray),  $A=5\ \mu\text{W}/\text{m}^3$ . Zoom of Lagrangian mesh and tracked materials (top frame) and velocity field (bottom frame) at (b)  $t=6.4$  Myr, (c)  $t=16$  Myr, and (d)  $t=25$  Myr. Lagrangian mesh initially consists of regular, rectangular cells; distorted cells indicate progressive deformation of materials in model (mesh plotted at one third actual resolution; highly deformed cells are not plotted). Bold arrows indicate relative flow vectors in lower crust and isotherms (heavy black lines) at  $200^\circ\text{C}$  intervals, starting at  $100^\circ\text{C}$  are plotted. (e) Topography along 250 km of surface, starting at left side of box.

cept in this case the radioactive block is centered above the downwelling so the convergent mobile crust accumulates and thickens at the downwelling. The horizontal extent of the uplifted region is approximately 50 km, roughly equal to that of the radioactive zone (Fig. 6e).

The thickened radioactive crust becomes increasingly hot, reaching temperatures of  $\sim 800^\circ\text{C}$ , thereby further weakening the ductile crust. Consequently, significant flow begins in this region (Fig. 6c) and the crust thins by outward channel flow of the hot low-viscosity lower crust above the downwelling plume (Fig. 6c). This style of localized channel flow is similar to that predicted to occur beneath plateaus at continental collision [42] and illustrates the feedback effects between radioactive heating of thickened crust and gravitationally driven channel flow. The channel flow would be even more pronounced were the effect of crustal melting in lowering the bulk effective viscosity of the hot thickened crust taken into account.

The variations of the surface topography, crustal thickness and Moho temperature above the center of the downwelling and radioactive block (i.e.,  $x=0$ ) are plotted versus time (Fig. 7). For the first 5 Myr the crust remains moderately strong. It undergoes a short period of surface uplift, then subsidence under the effect of the mantle lithosphere downwelling. The crust is progressively heated, up to temperatures of  $\sim 800^\circ\text{C}$ , causing weakening of the lower crust and underlying mantle (Fig. 6c). Consequently, the basal mantle forcing entrains the ductile lower crust towards the downwelling, thickening the crust to  $\sim 45$  km and leading to surface uplift (despite the downward mantle dynamical forcing).

The crustal thickening does not persist, but instead by  $\sim 15$  Myr the increasingly hot orogenic crustal region begins to undergo gravitationally driven extension and thinning (Fig. 6b,c) and from 20 Myr the surface subsides as the crust deflates. The decrease in surface elevation is relatively modest as the mantle lithosphere downwelling is still actively entraining a significant amount of lower crust material towards the center of the thickening above the downwelling (e.g., note inward-directed flow of crust beneath the outward

channel flow of radioactive crust, Fig. 6c,d). Consequently, the deflated crust does not return to its original thickness (30 km), but remains at a thickness of  $\sim 40$  km (Fig. 7b). Radioactive self-heating of the crust causes an overall rise in Moho temperature through the experiment while long timescale fluctuations (i.e., the relative temperature highs at  $\sim 7$  and 23 Myr) are due to changes in the heat flux at the base of the crust caused by the time-dependent mantle lithosphere downwelling.

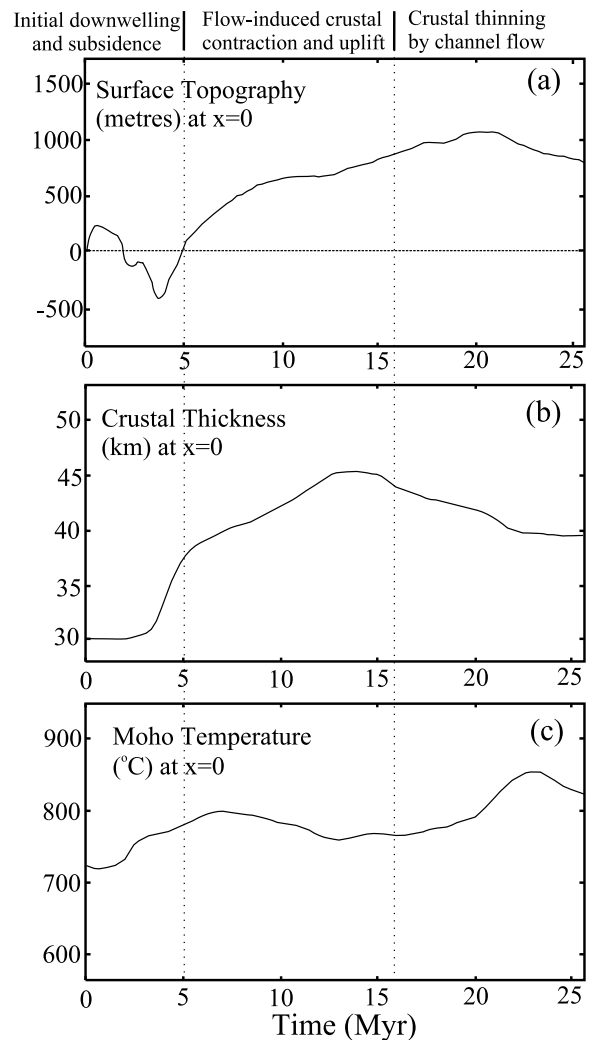


Fig. 7. Time series for: (a) surface topography at  $x=0$ , (b) crustal thickness at  $x=0$ , and (c) temperature at the base of the crust at  $x=0$  for radioactive crust model shown in Fig. 6.

A similar experiment was conducted in which the width of the radioactive zone in the crust was increased to 500 km (Fig. 8). The broad zone of radioactive crust causes thermal weakening of the crust on a regional scale. As the mantle lithosphere instability develops, it rapidly entrains the hot lower crustal material to the convergent zone, resulting in progressive crustal thickening above the downwelling (Fig. 8b). Crustal convergence also thickens the lower crustal radioactive region which self heats and eventually becomes hot and weak and outward flow of the low-viscosity lower crust commences by 6.4 Myr (Fig. 8c). In this case the overlying crust is also unstable and outward Couette flow results in subsequent thinning of the upper crust above the mantle lithosphere downwelling.

The progression of these events is similar to the previous model (Fig. 6) except for two main aspects. Firstly, the timescale for surface uplift and crustal thickening is significantly shorter because the wide radioactive region provides a larger volume of hot/weak lower crustal material that can be entrained towards the mantle flow-induced convergent zone. A peak topography and maximum crustal thickness is reached within  $\sim 5$  Myr from the start of the experiment and crustal thinning begins by  $\sim 5$  Myr (Fig. 9). Secondly, the broad radioactive lower crust influences the width of the surface topography features that develop in response to the mantle–crust tectonics (Fig. 8e) because the weak crust is essentially unconfined. In this model the weak crust thickens and uplifts quickly (Fig. 9) and consequently there is a sig-

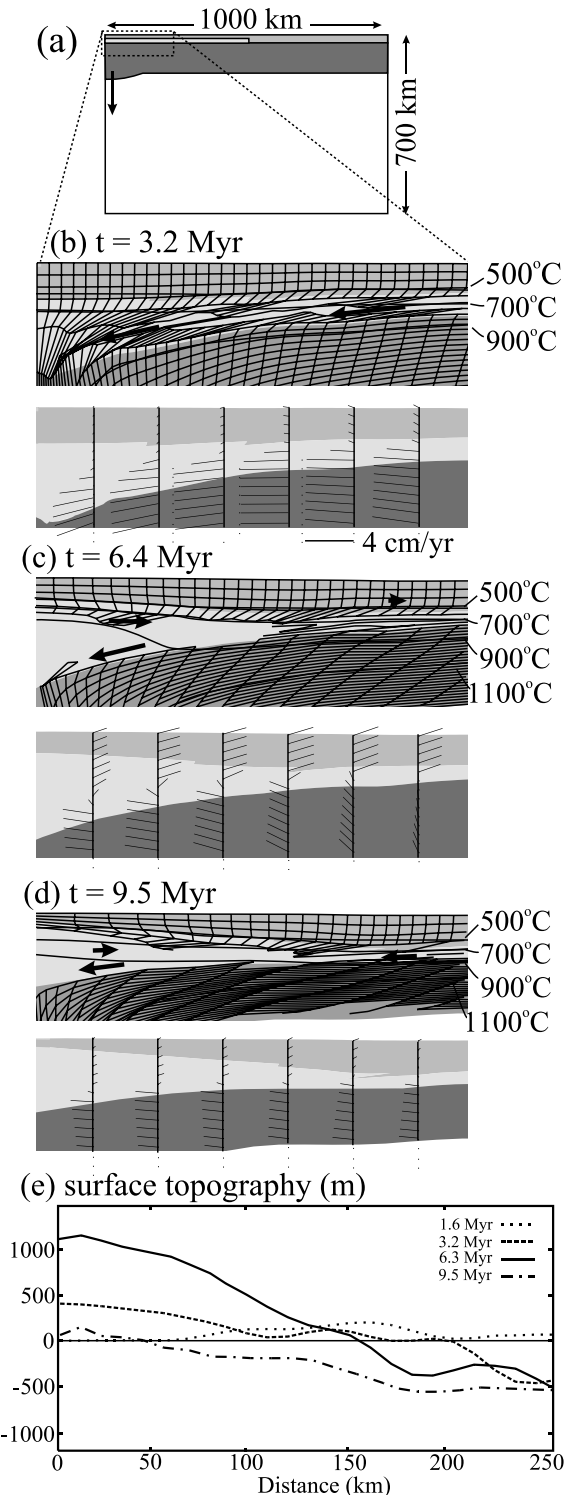


Fig. 8. Progressive deformation of crust in model with gravitational instability and wide zone of radioactive crust. (a) Initial model geometry; 15 km thick, 500 km wide radioactive region in lower crust (light gray),  $A = 5 \mu\text{W}/\text{m}^3$ . Zoom of Lagrangian mesh and tracked materials (top frame) and velocity field (bottom frame) at (b)  $t = 3.2$  Myr, (c)  $t = 6.4$  Myr, and (d)  $t = 9.5$  Myr. Lagrangian mesh initially consists of regular, rectangular cells; distorted cells indicate progressive deformation of materials in model (mesh plotted at one third actual resolution; highly deformed cells are not plotted). Bold arrows indicate relative flow vectors in lower crust and isotherms (heavy black lines) at  $200^\circ\text{C}$  intervals, starting at  $500^\circ\text{C}$  are plotted. (e) Topography along 250 km of surface, starting at left side of box.

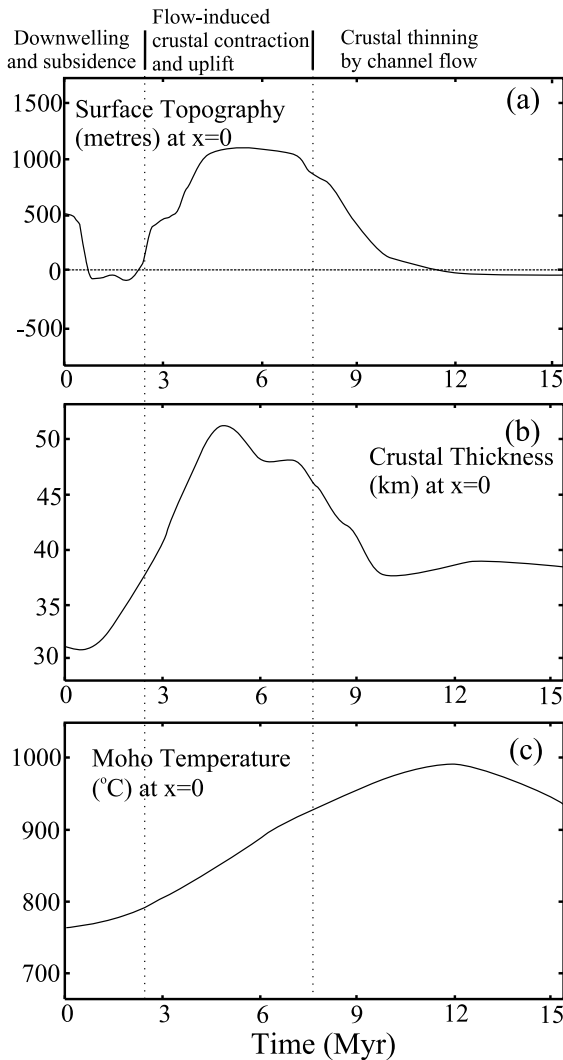


Fig. 9. Time series for: (a) surface topography at  $x=0$ , (b) crustal thickness at  $x=0$ , and (c) temperature at the base of the crust at  $x=0$  for wide radioactive crust model shown in Fig. 8.

nificantly reduced phase of initial surface subsidence (e.g., compared to Fig. 7a). Taking into account the symmetry of the solution space, a transient topographic high of  $\sim 150$  km half-width develops above the mantle downwelling (Fig. 8e). This is broader than the peak that developed with the narrow radioactive zone,  $\sim 50$  km (Fig. 6e). However, the high is significantly narrower than the 500 km half-width of the radioactive zone. This result indicates that for wide

regions of weakened crust the length scale of deformation and surface uplift (Fig. 8e) is controlled by the width of the mantle downwelling in contrast with narrow regions which control their own length scale (Fig. 6e).

### 3. Conclusions and discussion

The results of the numerical experiments have the following implications.

- The presence of crustal radioactive heating may make otherwise strong, tectonically inactive lithosphere in a continental interior susceptible to significant deformation induced by underlying mantle flow. Essentially, localized enrichments of radioactive elements may prepare the lithosphere for intraplate tectonic deformation and represent a primary control on the way the strength of the crust evolves during sub-crustal forcing.
- The feedback between thermal–mechanical processes during the evolution of the radioactive crust in response to a driving mantle downwelling event can cause the crust to go through phases of: (1) dynamic subsidence of strong crust, potentially forming intracratonic sedimentary basins; (2) flow-induced contraction, thickening and uplift of the self-heating crust; and (3) orogenic deflation as spontaneous crustal extension/thinning and surface subsidence occur. The extension may occur by channel flow confined to the mid/lower crust or may include the upper crust. Strong homogeneous crust subsides dynamically above mantle downwellings and undergoes essentially no internal deformation.
- The vertical distribution of radioactive elements in the crust is important, because buried sources of radioactive heating are more effective at heating/weakening the crust than those nearer the surface.
- A broad zone of deformation and surface uplift may develop in crust having a wide regional concentration of radioactive material in the lower crust, compared to a restricted topographic high above a localized concentration of radioactive elements. In the former case,

the width of the zone of high topography and thickened crust is limited by the width of the downwelling, rather than the horizontal extent of the region of radioactive crust.

The modeling results have particular implications for situations where the positive feedback between crustal tectonics and radioactive heating leading to enhanced deformation is the strongest. McLaren et al. [21] have proposed that the tectonic evolution of the Mt. Isa region of Australia in the Proterozoic is closely related to changes in the thermal state of the crust. In particular, they suggest that the burial of highly radioactive granites (e.g., having a present-day regional average  $A = 5.2 \mu\text{W}/\text{m}^3$ ) beneath insulating sediments resulted in an increase in crustal temperature and an associated decrease in crustal strength, leading to a phase of intraplate compression and crustal thickening during the Isan orogeny. Our numerical experiments suggest that radioactive crustal heating during thickening may provide the requisite thermal weakening feedback to permit a pronounced crustal contraction, thickening and surface uplift even when orogeny is relatively weakly driven by lithospheric RT instabilities. In the Isan orogeny case the sediment blanketing may have enhanced the thermal weakening but such insulation may not be required in general if the downwelling alone can initiate crustal thickening. The effect of thermal insulation and self-heating by sediments that would isostatically deepen and fill the dynamical depressions predicted by the numerical experiments would, however, further enhance the positive feedback mechanism in the intracratonic basinal parts of the models and may promote basin inversion even in instances where the crust does not deform in the current experiments.

For example, in the numerical models with a radioactive lower crust the surface topography above the mantle downwelling undergoes an inversion from subsidence to uplift (Figs. 5a and 7a). This reflects the evolution of the crust from the strong end-member to a thermally weakened state. While the crust is strong, it resists significant deformation and experiences intraplate subsidence induced by the downwelling RT instability. This process has been invoked, for example,

to account for certain phases of the formation of intracratonic basins such as the Ordovician and Silurian development of the Canning Basin in Western Australia [43]. Our results suggest that locations of crustal weakening (e.g., crust having high radioactive heat production or at weak pre-existing tectonic rifts) within such a basin may be susceptible to inversion and deformation during or subsequent to the flow-induced regional subsidence.

If the radioactive elements are distributed evenly through the entire crust or concentrated at depth, the crust is more prone to deformation induced by the underlying mantle lithosphere instability. This situation most closely corresponds to juvenile, undifferentiated crust [44–46]. Furthermore, it may be inferred that the coupled mantle–crust processes occurring in the models may play a role in the progressive cratonization of juvenile crust in an intraplate environment. That is, crust containing a uniform distribution of radioactive elements, or a concentration at depth, may promote intraplate tectonics through the feedback between mantle downwellings, crustal thickening, radioactive self-heating, melting and granitic diapirism which will lead to the concentration and upward transfer of radioactive elements in the crust.

In the experiments, we have made the assumption that the subcontinental mantle lithosphere is gravitationally unstable resulting in RT instabilities, thereby creating a mechanism that forces intraplate deformation. Houseman et al. [47] first proposed that during continental plate convergence, dense thickened mantle lithosphere is gravitationally unstable, and under certain conditions may develop as an RT-type mantle downwelling. This type of convective removal of the mantle lithosphere has been invoked to explain the geodynamic evolution in various tectonic environments [48–53]. The development of perturbations at the base of the lithosphere into gravitational instabilities requires that the rate of growth of the instabilities exceeds the dissipative effects of thermal diffusion. The growth rates of RT instabilities can be strongly affected by rheological variations such as temperature dependence [54,55] and non-linear viscosity [35,36]. Our models sug-

gest that with a power-law viscous rheology based on dry olivine for the mantle the lower portion of the mantle lithosphere is susceptible to RT instability for the assumed thermal structure of the lithosphere (Fig. 2). Even RT instability of just these lower regions of the mantle lithosphere can be sufficient to drive appreciable crustal tectonics in the experiments. However, in the models we ignore the influence of chemical alterations in the mantle lithosphere and potential associated buoyancy effects. These may be important for increasing the stability of the lithospheric roots [56,57] and inhibit the growth of RT instabilities at the base of the lithosphere.

The development of RT instabilities of the mantle lithosphere also requires that at least a portion of the mantle lithosphere is more dense than the underlying asthenosphere. Recent studies using mantle xenoliths/xenocrysts have placed constraints on the secular variation in the density of sub-crustal lithosphere through Earth history [58,59]. These analyses are interpreted to imply that there has been a progressive geochemical evolution from depleted mantle lithosphere in the Archean to a more fertile state in the Phanerozoic. Based on these measurements and assumed geotherms at past geological times, it is suggested that the cratonic mantle lithosphere in the Archean and Proterozoic may have been less dense than the underlying asthenosphere and it is only since the Phanerozoic, and below cool cratons that the mantle lithosphere is denser than the asthenosphere. The analyses in these studies considered the density structure of cratonic mantle lithosphere that has survived since the Archean and thus are inherently biased towards stable portions of the lithosphere. Nevertheless the results suggest potentially important implications for the secular change in behavior of mantle lithosphere roots.

In our experiments, we have only considered a mantle lithosphere instability/downwelling as the forcing for deformation of the radioactive intra-plate crust. As stated in Section 1, another mechanism which may act independently, or in concert with the flow-induced deformation in a plate interior is the effect of in-plane horizontal stresses acting on the margins of the plate. This has been proposed as a mechanism for vertical intraconti-

ental motions as pre-existing elastic lithospheric deflections may be amplified by horizontal compressive stresses, resulting in relative motions of uplift and subsidence of disparate regions of the continent [60–62]. The compressive stresses are associated with the movement of lithospheric plates and are transmitted from the margins of the plate to the interior. Flow-induced crustal deformation and topography, such as demonstrated in our numerical model experiments, may contribute the initial lithospheric perturbations that are then amplified by the in-plane stresses. Compressive stresses within the lithosphere may be expected to amplify the predicted time-dependent topography both by plate buckling, when the lithosphere is relatively strong, and/or by contraction and thickening of the weak radioactively heated crust. In addition, horizontal shortening of the plate may influence the growth rate and wavelength of the RT mantle lithosphere instability [34,36].

We have shown that there are potentially significant feedbacks between thermal and mechanical processes in the crust in response to driving by mantle downwelling. In the absence of superimposed effects from far-field in-plane lithospheric stresses, the character of the tectonic response can range from formation of intracratonic sedimentary basins to crustal thickening and orogenesis which may be followed by outward crustal flow. The particular response predicted for the crust above the downwelling is very sensitive to its strength, which is parameterized in terms of temperature caused by radioactive heating in the model experiments. Natural examples of the same coupled processes should be characterized by relatively short ( $< \sim 10$  Myr), moderate amplitude (few km), spatially restricted (few 100 km), pulse-like, tectonic events dictated by the space and timescale of the RT mantle lithosphere instability or zonation of weak crust/upper mantle lithosphere, and the requirement that the lithosphere be susceptible to RT instabilities.

## Acknowledgements

The work was funded by research grants to

R.N.P. and C.B. from the Natural Sciences and Engineering Research Council of Canada. C.B. also acknowledges support through the Inco Fellowship of the Canadian Institute for Advanced Research and through the Canada Research Chair in Geodynamics. Numerical calculations used software developed by Philippe Fullsack. We thank the reviewers, Julian Lowman and Greg Houseman, for constructive comments on the original manuscript. *[SK]*

## References

- [1] D.P. McKenzie, J.M. Roberts, N.O. Weiss, Convection in the Earth's mantle: towards a numerical solution, *J. Fluid Mech.* 62 (1974) 465–538.
- [2] D.P. McKenzie, Surface deformation, gravity anomalies and convection, *GJRS* 48 (1977) 211–238.
- [3] C. Lithgow-Bertelloni, P.G. Silver, Dynamic topography, plate driving forces and the African superswell, *Nature* 395 (1998) 269–272.
- [4] M. Gurnis, J.X. Mitrovica, J. Ritsema, H.J. van Heijst, Constraining mantle structure using geological evidence of surface uplift rates: The case of the African Superplume, *Geochem. Geophys. Geosyst.* (2000) 1999GC-000035.
- [5] J.X. Mitrovica, C. Beaumont, G.T. Jarvis, Tilting of continental interiors by the dynamical effects of subduction, *Tectonics* 8 (1989) 1079–1094.
- [6] M. Gurnis, Rapid continental subsidence following the initiation and evolution of subduction, *Science* 255 (1992) 1556–1558.
- [7] M. Russell, M. Gurnis, The planform of epeirogeny: vertical motions of Australia during the Cretaceous, *Basin Res.* 6 (1994) 63–76.
- [8] T.A. Stern, W.E. Holt, Platform subsidence behind an active subduction zone, *Nature* 368 (1994) 233–236.
- [9] D.L. Bindschadler, E.M. Parmentier, Mantle flow tectonics: The influence of a ductile lower crust and implications for the formation of topographic uplands on Venus, *J. Geophys. Res.* 95 (1990) 21329–21344.
- [10] A. Lenardic, W.M. Kaula, D.L. Bindschadler, A mechanism for crustal recycling on Venus, *J. Geophys. Res.* 98 (1993) 18697–18705.
- [11] A. Lenardic, W.M. Kaula, D.L. Bindschadler, Some effects of a dry crustal flow law on numerical simulations of coupled crustal deformation and mantle convection on Venus, *J. Geophys. Res.* 100 (1995) 16949–16957.
- [12] S.E. Smrekar, E. Parmentier, The interaction of mantle plumes with surface thermal and chemical boundary layers: Applications to hotspots on Venus, *J. Geophys. Res.* 101 (1996) 5397–5410.
- [13] L. Fleitout, C. Froidevaux, Tectonics and topography for a lithosphere containing density heterogeneities, *Tectonics* 1 (1982) 21–56.
- [14] A.M. Marotta, M. Fernandez, R. Sabadini, The onset of extension during lithospheric shortening: A two-dimensional thermomechanical model for lithospheric unrooting, *Geophys. J. Int.* 139 (1999) 98–114.
- [15] E.A. Neil, G.A. Houseman, Rayleigh–Taylor instability of the upper mantle and its role in intraplate orogeny, *Geophys. J. Int.* 138 (1999) 89–107.
- [16] S. Zhong, Dynamics of crustal compensation and its influences on crustal isostasy, *J. Geophys. Res.* 102 (1997) 15287–15299.
- [17] L. Moresi, A. Lenardic, Three-dimensional numerical simulations of crustal deformation and subcontinental mantle convection, *Earth Planet. Sci. Lett.* 150 (1997) 233–243.
- [18] L. Moresi, A. Lenardic, Three-dimensional mantle convection with continental crust: First-generation numerical simulations, *Earth Interact.* 3 (1999) 1–14.
- [19] R.N. Pysklywec, J.X. Mitrovica, M. Ishii, Mantle avalanche as a driving force for tectonic reorganization in the southwest Pacific, *Earth Planet. Sci. Lett.* 209 (2003) 29–38.
- [20] D.L. Kohlstedt, B. Evans, S.J. Mackwell, Strength of the lithosphere: Constraints imposed by laboratory experiments, *J. Geophys. Res.* 100 (1995) 17587–17602.
- [21] S. McLaren, M. Sandiford, M. Hand, High radiogenic heat-producing granites and metamorphism – an example from the western Mount Isa inlier, Australia, *Geology* 27 (1999) 679–682.
- [22] R.D. Shaw, M.A. Etheridge, K. Lambeck, Development of the late Proterozoic to mid-Palaeozoic intracratonic Amadeus Basin in central Australia: A key to understanding tectonic forces in plate interiors, *Tectonics* 10 (1991) 688–721.
- [23] M.G. O'Dea, G.S. Lister, T. MacCready, P.G. Betts, N.H.S. Oliver, K.S. Pound, W. Huang, R.K. Valenta, Geodynamic evolution of the Proterozoic Mount Isa terrain, in: J.P. Burg, M. Ford (Eds.), *Orogeny Through Time*, *Geol. Soc. Spec. Publ.* 121, 1997, pp. 99–122.
- [24] P.G. Betts, Palaeoproterozoic mid-basin inversion in the northern Mt. Isa terrane, Queensland, *Aust. J. Earth Sci.* 46 (1999) 735–748.
- [25] D.L. Scott, D.J. Rawlings, R.W. Page, C.Z. Tarlowski, M. Idnurm, M.J. Jackson, P.N. Southgate, Basement framework and geodynamic evolution of the Palaeoproterozoic superbasins of north-central Australia: an integrated review of geochemical, geochronological and geophysical data, *Aust. J. Earth Sci.* 47 (2000) 341–380.
- [26] M. Sandiford, M. Hand, Controls on the locus of intraplate deformation in central Australia, *Earth Planet. Sci. Lett.* 162 (1998) 97–110.
- [27] S. McLaren, M. Sandiford, Long-term thermal consequences of tectonic activity at Mt. Isa: implications for polyphase tectonism in the Proterozoic, *Geol. Soc. Spec. Publ.* 184 (2001) 219–236.

- [28] M. Sandiford, S. McLaren, Tectonic feedback and the ordering of heat producing elements within the continental lithosphere, *Earth Planet. Sci. Lett.* 204 (2002) 133–150.
- [29] P. Fullsack, An arbitrary Lagrangian–Eulerian formulation for creeping flows and applications in tectonic models, *Geophys. J. Int.* 120 (1995) 1–23.
- [30] G.C. Gleason, J. Tullis, A flow law for dislocation creep of quartz aggregates determined with the molten salt cell, *Tectonophysics* 247 (1995) 1–23.
- [31] F.A. Dahlen, Noncohesive critical Coulomb wedges: An exact solution, *J. Geophys. Res.* 89 (1984) 10125–10133.
- [32] C. Beaumont, P.J.J. Kamp, J. Hamilton, P. Fullsack, The continental collision zone, South Island, New Zealand: Comparison of geodynamical models and observations, *J. Geophys. Res.* 101 (1996) 3333–3359.
- [33] G. Hirth, D.L. Kohlstedt, Water in the oceanic upper mantle: Implications for rheology, melt extraction and the evolution of the lithosphere, *Earth Planet. Sci. Lett.* 144 (1996) 93–108.
- [34] C.P. Conrad, P. Molnar, The growth of Rayleigh–Taylor-type instabilities in the lithosphere for various rheological and density structures, *Geophys. J. Int.* 129 (1997) 95–112.
- [35] G.A. Houseman, P. Molnar, Gravitational (Rayleigh–Taylor) instability of a layer with non-linear viscosity and convective thinning of continental lithosphere, *Geophys. J. Int.* 128 (1997) 125–150.
- [36] P. Molnar, G.A. Houseman, C.P. Conrad, Rayleigh–Taylor-type instability and convective thinning of mechanically thickened lithosphere: Effects of non-linear viscosity decreasing exponentially with depth and of horizontal shortening of the layer, *Geophys. J. Int.* 133 (1998) 568–584.
- [37] G.A. Houseman, P. Molnar, Mechanisms of lithospheric rejuvenation associated with continental orogeny, in: I.S. Buick, M. Hand (Eds.), *Continental Reactivation and Reworking*, *Geol. Soc. Lond. Spec. Publ.* 184, London, 2001, pp. 13–38.
- [38] P.E. van Keken, S.D. King, H. Schmeling, U.R. Christensen, D. Neumeister, M.P. Doin, A comparison of methods for the modeling of thermochemical convection, *J. Geophys. Res.* 102 (1997) 22477–22496.
- [39] A. Poliakov, Y. Podladchikov, Diapirism and topography, *Geophys. J. Int.* 109 (1992) 553–564.
- [40] B. Blankenbach, F. Busse, U. Christensen, L. Cserepes, D. Gunkel, U. Hansen, H. Harder, G. Jarvis, M. Koch, G. Marquart, D. Moore, P. Olson, H. Schmeling, T. Schnaubelt, A benchmark comparison for mantle convection codes, *Geophys. J. Int.* 98 (1989) 23–38.
- [41] R.L. Rudnick, Thermal structure, thickness and composition of continental lithosphere, *Chem. Geol.* 145 (1998) 395–411.
- [42] C. Beaumont, R.A. Jamieson, M.H. Nguyen, B. Lee, Himalayan tectonics explained by extrusion of a low-viscosity crustal channel coupled to focused surface denudation, *Nature* 414 (2001) 738–742.
- [43] M.F. Middleton, A model for the formation of intracratonic sag basins, *Geophys. J. Int.* 99 (1989) 665–675.
- [44] R.L. Rudnick, Making continental crust, *Nature* 378 (1995) 571–578.
- [45] S.M. McLennan, S.R. Taylor, Heat flow and the chemical composition of continental crust, *J. Geol.* 104 (1996) 369–377.
- [46] F. Albarede, The growth of continental crust, *Tectonophysics* 296 (1998) 1–14.
- [47] G.A. Houseman, D.P. McKenzie, P. Molnar, Convective instability of a thickened boundary layer and its relevance for the thermal evolution of continental convergent belts, *J. Geophys. Res.* 86 (1981) 6115–6132.
- [48] P. England, G.A. Houseman, Extension during continental convergence, with application to the Tibetan Plateau, *J. Geophys. Res.* 94 (1989) 17561–17579.
- [49] J.P. Platt, R.L.M. Vissers, Extensional collapse of thickened continental lithosphere: A working hypothesis for the Alboran Sea and Gibraltar Arc, *Geology* 17 (1989) 540–543.
- [50] A.M. Marotta, M. Fernandez, R. Sabadini, Mantle unrooting in collisional settings, *Tectonophysics* 296 (1998) 31–46.
- [51] G.A. Houseman, E.A. Neil, M.D. Kohler, Lithospheric instability beneath the Transverse Ranges of California, *J. Geophys. Res.* 105 (2000) 16237–16250.
- [52] C.T. Lee, Q. Yin, R.L. Rudnick, J.T. Chesley, S.B. Jacobsen, Os isotopic evidence for mesozoic removal of lithospheric mantle beneath the Sierra Nevada, California, *Science* 289 (2000) 1912–1916.
- [53] V. Levin, J. Park, M.T. Brandon, W. Menke, Thinning of the upper mantle during late Paleozoic Appalachian orogenesis, *Geology* 28 (2000) 239–242.
- [54] W.R. Buck, M.N. Toksöz, Thermal effects of continental collisions: Thickening a variable viscosity lithosphere, *Tectonophysics* 100 (1983) 53–69.
- [55] A. Lenardic, W.M. Kaula, More thoughts on convergent crustal plateau formation and mantle dynamics with regard to Tibet, *J. Geophys. Res.* 100 (1995) 15193–15203.
- [56] A. Lenardic, L.N. Moresi, Some thoughts on the stability of cratonic lithosphere: Effects of buoyancy and viscosity, *J. Geophys. Res.* 104 (1999) 12747–12758.
- [57] C.T. Lee, Q. Yin, R.L. Rudnick, S.B. Jacobsen, Preservation of ancient and fertile lithospheric mantle beneath the southwestern United States, *Nature* 411 (2001) 69–73.
- [58] Y.H.P. Djomani, S.Y. O’Reilly, W.L. Griffin, P. Morgan, The density structure of subcontinental lithosphere through time, *Earth Planet. Sci. Lett.* 184 (2001) 605–621.
- [59] S.Y. O’Reilly, W.L. Griffin, Y.H.P. Djomani, P. Morgan, Are lithospheres forever? Tracking changes in subconti-

- mental lithospheric mantle through time, *GSA Today* 11 (2001) 4–10.
- [60] K. Lambeck, The role of compressive forces in intracratonic basin formation and mid-plate orogenies, *Geophys. Res. Lett.* 10 (1983) 843–886.
- [61] S. Cloetingh, H. McQueen, K. Lambeck, On a tectonic mechanism for regional sea level variations, *Earth Planet. Sci. Lett.* 75 (1985) 157–166.
- [62] S. Cloetingh, Intraplate stresses: A new tectonic mechanism for fluctuations of relative sea level, *Geology* 14 (1986) 617–620.